JOURNAL OF GEOPHYSICAL RESEARCH, VOL. 108, NO. A11, 1393, doi:10.1029/2003JA009826, 2003

Near-source and remote observations of kilometric continuum radiation from multispacecraft observations

J. D. Menietti, R. R. Anderson,[1] J. S. Pickett, and D. A. Gurnett
Department of Physics and Astronomy, University of Iowa, Iowa City, Iowa, USA

H. Matsumoto
Radio Science Center for Space and Atmosphere, Kyoto University, Uji, Japan

Received 2 January 2003; revised 29 July 2003; accepted 14 August 2003; published 14 November 2003.

[1] Kilometric continuum (KC) radiation was first identified from Geotail plasma wave observations. Past authors have shown that this emission has a frequency range that overlaps that of the auroral kilometric radiation (AKR) but is characterized by a fine structure of narrow-bandwidth, linear features that have nearly constant or drifting frequency. This fine structure is distinct from that of AKR. KC also apparently has a distinct source region probably associated with the low-latitude inner magnetosphere, consistent with direction-finding and ray-tracing results. We present new high-resolution electric and magnetic field observations of KC obtained by the Polar plasma wave instrument in the near-source region. These observations show intense electrostatic and less intense electromagnetic emissions near the magnetic equator at the plasmapause. Simultaneously, Geotail, located at 20 to 30 R_E in radial distance, observes KC in the same frequency range. These data support a possible mode-conversion source mechanism near a region of high-density gradient. High-resolution data obtained from wideband receivers on board both Polar and Cluster show closely spaced bands of emission near the magnetic equator that may be due to many nearby independent sources of EM emission perhaps associated with density fluctuations or cavities in the plasmasphere. *INDEX TERMS:* 2772 Magnetospheric Physics: Plasma waves and instabilities; 2740 Magnetospheric Physics: Magnetospheric configuration and dynamics; 2768 Magnetospheric Physics: Plasmasphere; 6984 Radio Science: Waves in plasma; *KEYWORDS:* plasma waves and instabilities

Citation: Menietti, J. D., R. R. Anderson, J. S. Pickett, D. A. Gurnett, and H. Matsumoto, Near-source and remote observations of kilometric continuum radiation from multispacecraft observations, *J. Geophys. Res.*, *108*(A11), 1393, doi:10.1029/2003JA009826, 2003.

1. Introduction

[2] *Brown* [1973] and *Gurnett and Shaw* [1973] first reported terrestrial nonthermal continuum emission in a broad frequency range extending from ~5 kHz to < 100 kHz. The term continuum implied a diffuse, rather continuous spectrum. *Gurnett and Shaw* [1973] and *Gurnett* [1975] proposed a source near the dawnside plasmapause, with a source mechanism associated with intense upper hybrid waves. *Kurth et al.* [1981] and *Kurth* [1982] [cf. *Oya et al.*, 1991] described the details of the narrow-banded escaping component of continuum emission (ordinary mode), providing clear evidence of its narrow-bandedness associated with intense upper hybrid (UH) resonance emissions. These emissions are also believed to have a low-latitude source in the outer plasmasphere and in the magnetopause [*Morgan and Gurnett*, 1991]. The source mechanism of this continuum emission has been proposed to be a mode conversion process occurring near the dayside magnetopause and/or the nightside plasmapause near the equator. Both linear [e.g., *Jones*, 1976, 1988; *Budden*, 1980] and nonlinear [cf. *Melrose*, 1981; *Fung and Papadopoulos*, 1987; *Rönnmark*, 1983] classes of mode conversion have been suggested as summarized by *Kurth* [1992].

[3] *Hashimoto et al.* [1999] have described kilometric continuum (KC) as emission that lies in the same frequency range as auroral kilometric radiation (AKR) [cf. *Gurnett*, 1974] but with a different spectral morphology and a unique source region, the low-latitude inner plasmasphere. KC was observed by Geotail (in an equatorial orbit) to consist of slowly drifting narrowband signals in the frequency range 100 kHz < f < 800 kHz. Direction-finding using spin modulation of the emission at 400 kHz indicated the source of the emission is consistent with the low-magnetic-latitude inner plasmasphere. The emission thus has much in common with nonterrestrial continuum emission observed at lower frequencies (typically <100 kHz). More recently, *Green et al.* [2002a, 2002b] have shown an

[1]Also at Radio Science Center for Space and Atmosphere, Kyoto University, Uji, Japan.

0148-0227/03/2003JA009826$09.00

association of the kilometric continuum with plasmaspheric notches (bite-outs) of density and suggested that these large-structure cavities may be a source region of the KC. As pointed out by *Hashimoto et al.* [1999], KC emission was probably observed in the past, but not identified as a distinct component of continuum emission [cf. *Kurth et al.*, 1981].

[4] In this paper we show joint observations of Polar and Geotail plasma wave data. Geotail observes KC at distances >10 R_E, while Polar passes through the magnetic equator near the plasmapause and the proposed source region of KC. In addition we include some unique, high-resolution data obtained by the wideband receivers on board both Polar and the Cluster spacecraft that provide new and interesting information regarding the source region and possible density structure of the outer low-latitude plasmasphere.

2. Instrumentation

2.1. Polar

[5] The Polar satellite was launched in late February 1996 into a polar orbit with apogee of about 9 R_E and a perigee of about 1.8 R_E. Polar is the first satellite to have three orthogonal electric antennas (E_u, E_v, and E_z), three triaxial magnetic search coils, and a magnetic loop antenna, as well as an advanced plasma wave instrument [*Gurnett et al.*, 1995]. This combination can potentially provide the polarization and direction of arrival of a signal without any prior assumptions.

[6] The Plasma Wave Instrument on the Polar spacecraft is designed to provide measurements of plasma waves in the Earth's polar regions over the frequency range from 0.1 Hz to 800 kHz. Five receiver systems are used to process the data: a wideband receiver, a high-frequency waveform receiver (HFWR), a low-frequency waveform receiver, two multichannel analyzers, and a pair of sweep frequency receivers (SFR). For the high-frequency emissions of interest here, the SFR is of special interest. The SFR has a frequency range from 24 Hz to 800 kHz in five frequency bands. The frequency resolution is about 3% at the higher frequencies. In the log mode a full frequency spectrum can be obtained every 33 s. From 12.5 to 800 kHz, of interest in this study of KC, a full frequency spectrum can be obtained every 2.4 s.

[7] The wideband receiver (WBR) provides high-resolution waveform data and is programmable allowing the selection of 11, 22, or 90 kHz bandwidths with a lower band edge (base frequency) at 0, 125, 250, and 500 kHz. In the 90 kHz bandwidth mode the sampling rate is 249 kHz.

2.2. Geotail

[8] Geotail was launched into a low-inclination orbit, and since February 1995 this orbit has been elliptical with a perigee of about 10 R_E and an apogee of about 30 R_E. The Sweep-Frequency Analyzer (SFA) on Geotail is comprised of eight receivers that measure the electric field over the range of 24 Hz < f < 800 kHz, and the magnetic field over the range 24 Hz < f < 12.5 kHz. In the KC frequency range there are two receivers. One operates in the range 12.5 kHz to 100 kHz in 680 Hz steps, and the other operates over the range 100 to 800 kHz in 5.4 kHz steps. The instrument uses two spin-plane electric dipole antennas with a tip-to-tip length of 100 m [cf. *Matsumoto et al.*, 1994].

2.3. Cluster

[9] The Cluster mission consists of four identical satellites in a high-inclination orbit with a nominal apogee of 19 R_E and perigee of 4 R_E. The mission objectives include studies of the magnetopause and magnetotail reconnection sites and magnetospheric phenomena.

[10] The wideband plasma wave investigation on Cluster is part of the Wave Experiment Consortium (WEC), which consists of five instruments designed specifically to study magnetospheric wave phenomena [*Pedersen et al.*, 1997]. The Cluster mission and wideband instrument have been described in previous publications [cf. *Gurnett et al.*, 2001]. The objective of the wideband plasma wave investigation is to provide very high-time frequency resolution measurements in order to resolve spatial and temporal structure in the plasma waves and magnetosphere. The investigation consists of four identical instruments (one on each spacecraft) called the Wideband (WBD) plasma wave instruments. These instruments measure electric or magnetic field waveforms in one of three possible bandwidths: 25 Hz to 9.5 Hz, 50 Hz to 19 kHz, or 1 kHz to 75 kHz. The base frequency (frequency offset) can be programmed to be 0, 125 kHz, 250 kHz, or 500 kHz. The bit rate in the real time mode of operation is 220 kbits/s.

3. Observations

[11] We have examined a large portion of the Polar SFR data and the Geotail SFA data for examples of possible encounters with KC emissions. The orbits of the two satellites during 1996–1997 made these two instruments particularly well suited for a joint study. Polar was placed in a 90-degree inclination orbit with an apogee of about 9 R_E and a perigee of about 1.8 R_E. The orbital period is about 18 hours. Polar passed through the nightside equatorial region near the plasmapause (4–5 R_E), and at somewhat lower distances (2.5–3.5 R_E) on the dayside during the period of analysis in this study. During this period the apogee was over the northern polar cap and perigee over the southern polar region. The Geotail satellite orbit during 1996 to 1997 was in an equatorial orbit with a nightside apogee of about 30 R_E and a dayside perigee of about 10 R_E, and the orbital period was about 1.5 days. The purpose of the present study was to investigate observations of kilometric continuum emission (KC) observed by both satellites, particularly simultaneous observations. The orbit of Polar brought it near the proposed source region of KC, near the equatorial plasmapause [*Hashimoto et al.*, 1999; *Green et al.*, 2002a].

[12] We have chosen a number of interesting examples to display. These cases represent times when the Polar PWI detected electromagnetic (EM) emission near the upper hybrid frequency, f_{UH}, generally when the spacecraft was near the magnetic equator. This is not a comprehensive study of all of the equator passes but does represent a sizeable sampling of the data.

[13] We start with data from 20 May 1996, when Polar at lower altitude and Geotail at higher altitude are simultaneously monitoring the same magnetic local time (MLT). In Figure 1 we display a frequency-time spectrogram of the

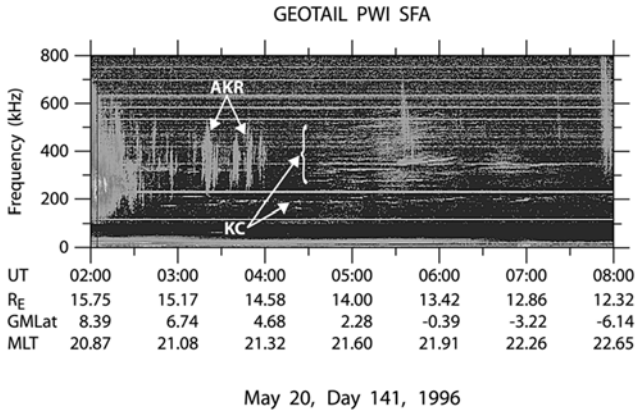

Figure 1. In Figure 1 we display a frequency-time spectrogram of the Geotail plasma wave instrument (PWI) sweep-frequency analyzer (SFA) with relative power gray-coded. This spectrogram covers a 6-hour period on 20 May 1996, when the spacecraft was on the nightside at a distance ranging from 15.75 R_E to 12.3 R_E, and ranging in magnetic latitude from 8.4° through the magnetic equator to −6.1°. The kilometric continuum emission is seen as the narrow-band frequency-drifting features indicated.

Geotail plasma wave instrument sweep-frequency analyzer with relative power gray-coded. This spectrogram covers a 6-hour period when the spacecraft was on the nightside at a distance ranging from 15.75 R_E to 12.3 R_E and ranging in magnetic latitude from 8.4° through the magnetic equator to −6.1°. The near constant frequency fine structures extending in frequency from 100 kHz to over 600 kHz are kilometric continuum emission and are distinguished morphologically from the more broad-banded structures comprising the auroral kilometric radiation (AKR). Most of the KC emission is seen in the time interval from about 0430 to about 0700 and extends from approximately 175 kHz to well over 500 kHz. We will concentrate on a 30-min time period from 0340 to 0410 that is displayed in Figure 2a. Here we indicate both the AKR, the more broadbanded structures, and the much more narrow-banded and weak KC emission near 200 kHz. Note that both the AKR and the KC show a spin modulation. Geotail at this time is near a MLT of about 21.3 hours. The Polar PWI sweep-frequency receiver (SFR) data for a similar time period is shown in Figure 2b. Here the MLT is near 22 hours and the spacecraft varies in radial distance from 4.11 to 3.58 R_E. The magnetic latitude, λ_m, varies in the polar orbit from 15° to <4.7°. The top panel displays the electric field while the bottom panel shows the magnetic field data in a frequency range from 100 kHz to 250 kHz. We have chosen a gray scale to emphasize the most intense emissions, and often the magnetic oscillations disappear. These spectrograms show a banded electromagnetic emission with separation of the bands consistent with harmonics of the local electron cyclotron frequency, f_{ce}, which varies from about 12.5 to 19 kHz over this time range. We have overplotted a series of dashed lines with a frequency separation that varies linearly from 10 kHz at 0340 to 20 kHz at 0403. This emission could be KC near its source in the frequency range of 150 to 200 kHz.

[14] In Figure 3a we show a much higher resolution spectrogram that covers only 2 min of time. Here a spin modulation of the electric and magnetic field data is discernable. The spin period of the Polar satellite is about 6 seconds while the nulls in Figure 3a are about 10 s apart. This is due to an aliasing of the spin period with the instrument frequency cycling period of about 2.4 s. We have determined the angle between the PWI E_u antenna and the local magnetic field for this time period. The peaks in the electric field intensity occur when the antenna is nearly perpendicular to the ambient magnetic field, **B**, while the oscillating magnetic field intensity shown in the lower panel shows intensity maximum that are almost aligned with **B**. These observations are consistent with electrostatic upper hybrid emission and electromagnetic emission. This example is similar to numerous other examples of well-organized spin modulation data. We have calculated the ratio of B/E for the time interval of Figure 3a. Each set of points in Figure 3b corresponds to a subset of the time interval shown at the top of the figure. Each point is measured at a frequency channel of the Polar SFR. The frequency resolution is 1 kHz, and the dwell time on each frequency for a set of connected points is 36.8 ms. The time interval between each set of connected points is about 32 s. The lines serve only to connect the data points and do not imply intermediate values. The ratio varies considerably with frequency and time (Figure 3b) and is consistent with a mixture of both electrostatic and electromagnetic waves. We do not accurately know the plasma frequency, and we cannot with certainty delineate between wave modes. For some time intervals and $f \sim 165$ kHz, the ratio is $\lesssim 1$, suggestive of purely EM emission in the O, Z, or even X modes. For a cold plasma with f_p = 159.4 kHz, f_{ce} = 13.5 kHz, and wave normal angle of 88°, the index of refraction, N, for the O-mode and X-mode are $\lesssim 1$ for $f > f_p$. The Z-mode index of refraction is also $\lesssim 1$ for $f < f_p$. For example, for f = 168 kHz, N = 0.192 (X-mode); for f = 165 kHz, N = 0.258 (O-mode); for f = 159 kHz, N = 0.754 (Z-mode).

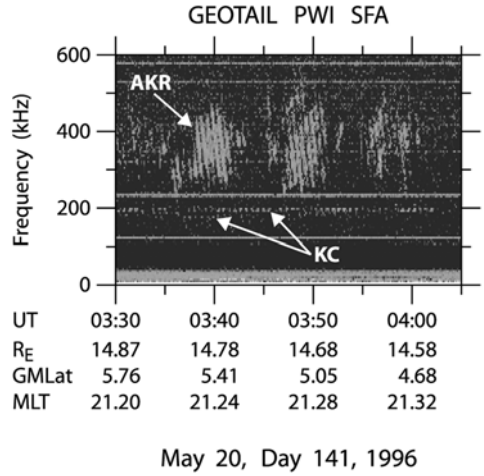

Figure 2a. A higher resolution spectrogram of the Geotail data shown in Figure 1, now for the time interval from 0330 to 0405. We indicate the narrow-band KC emission near 200 kHz. Note the spin-modulation of this emission which produces the periodic temporal enhancements of the banded emission.

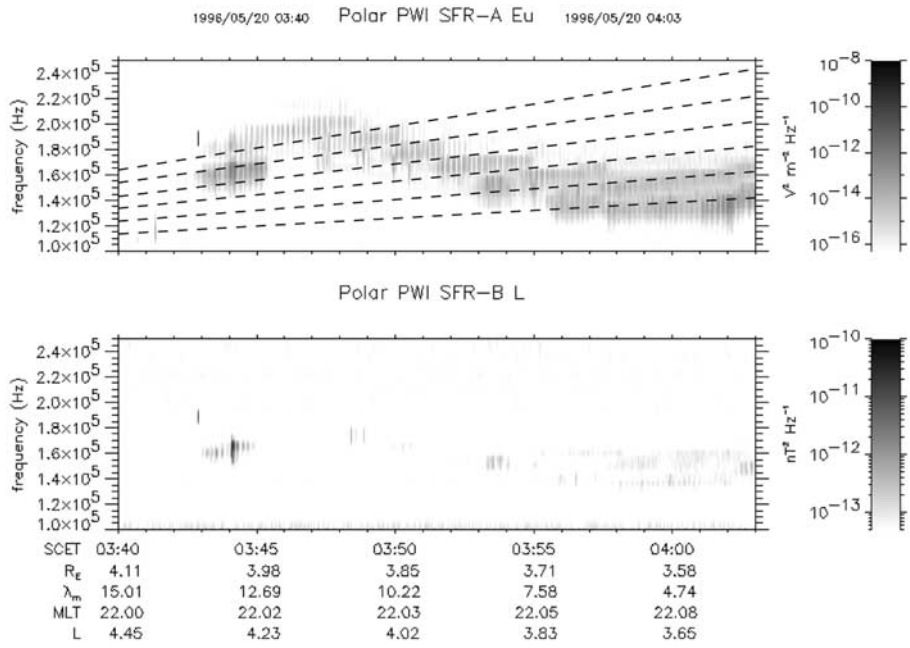

Figure 2b. A frequency-time spectrogram of the PWI sweep-frequency receiver for a twenty-five minute period of day 20 May 1996. Here the MLT is near 22 hours and the spacecraft varies in radial distance from 4.11 to 3.58 R_E. The magnetic latitude varies in the polar orbit from 15° to <4.7°. The top panel displays the electric field while the bottom panel shows the magnetic field data in a frequency range from 100 kHz to 250 kHz. The dashed lines are explained in the text.

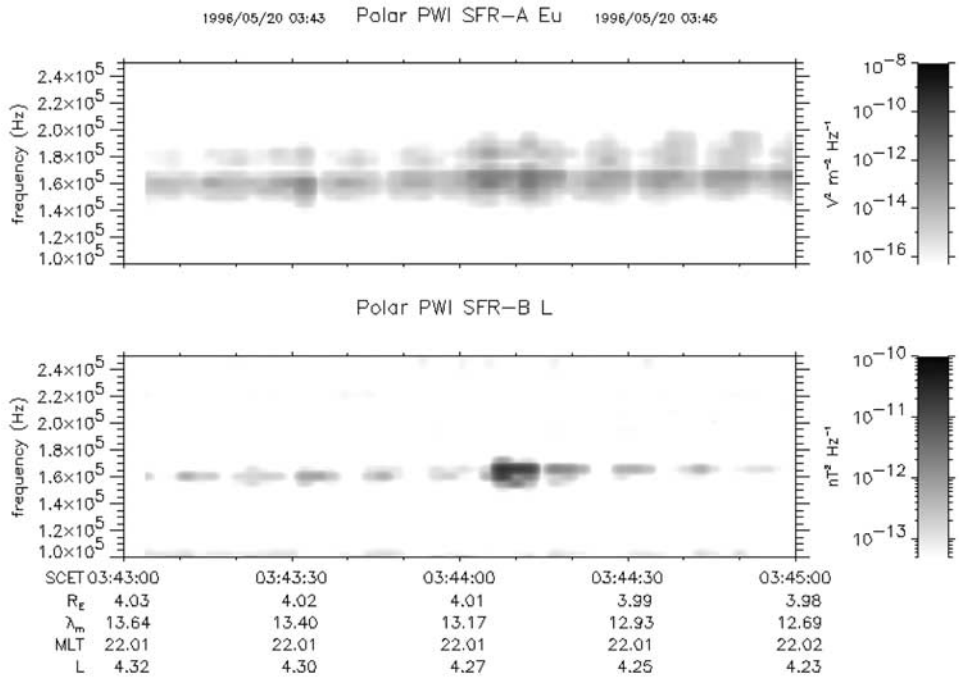

Figure 3a. A much higher resolution PWI spectrogram of day 20 May 1996 that covers only 2 min of time. Here a spin modulation of the electric and magnetic field data is discernable. The spin period of the Polar satellite is about 6 s while the nulls in Figure 3a are about 10 s apart. This is due to an aliasing of the spin period with the instrument frequency cycling period of about 2.5 s.

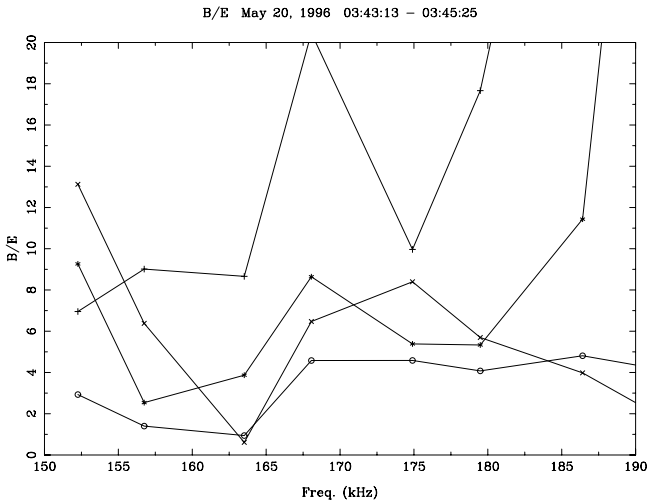

Figure 3b. A plot of B/E versus frequency for the time interval shown. Each set of points represents a different subinterval of the total time interval. The values become less than 1 (consistent with nearly pure EM emission) near $f = 165$ kHz times near 0343:20 and 0344:53. Elsewhere the values are larger indicative of a mixture of wave modes.

[15] In Figure 4a we show a spectrogram of Polar SFR data for a 1-hour period on day 11 February 1997. During this time period the spacecraft is located in the afternoon sector with MLT ranging from 15.0 hours to 16.1 hours. The radial distance varies from 2.11 R_E to 3.4 R_E. Significantly, the magnetic latitude varies from high-southern latitudes, $-38.2°$ through the magnetic equator to $\sim 14.4°$. The electric field data show a band of upper hybrid emission centered near 200 kHz with two regions of more enhanced emission near 1520 and $\lambda_m \sim -23.5°$ and again near the magnetic equator at about 1543 spacecraft event time (SCET). During both of these times the emission becomes electromagnetic as seen in the bottom panel. During this same time period, Geotail observed KC and was located in the MLT range of 15.9 hours $\lesssim$ MLT $\lesssim$ 16.2 hours, 14.3 R_E < R < 14.9 R_E, and $7.5° < \lambda_m < 10.4°$. Note that Geotail does not reach the high latitudes achieved by Polar but does observe KC within $\sim 10°$ of the magnetic equator. The KC emission is indicated in Figure 4b in the frequency range from 100 kHz to over 200 kHz (overlapping some of those frequencies observed by Polar in Figure 4a) where it becomes almost obscured by the more intense AKR. If the EM emission observed by Polar is KC, then it is observed at a magnetic latitude that is significantly higher than 10°. *Hashimoto et al.* [1999] reported that almost all KC emission is observed in the range of magnetic latitudes of $\pm 10°$, although some emission was reported as high as 20° (cf. their Figure 9).

[16] In Figure 5a we show Geotail observations for a ten hour period on 23 May 1996. The AKR and KC emissions are indicated. To compare with Polar observations we concentrate in Figure 5b on a much smaller period of time between 0208 and 0232. The KC shows a spin modulation and characteristic fine structure in the frequency range from 100 kHz < f < 200 kHz. Polar observations for the period from 0210 to 0232 are compared in Figure 6. We note that Geotail at this time is located at R $\sim$ 30.25 R_E, MLT $\sim$14.55 hours, and $\lambda_m \sim 13°$, while Polar was in

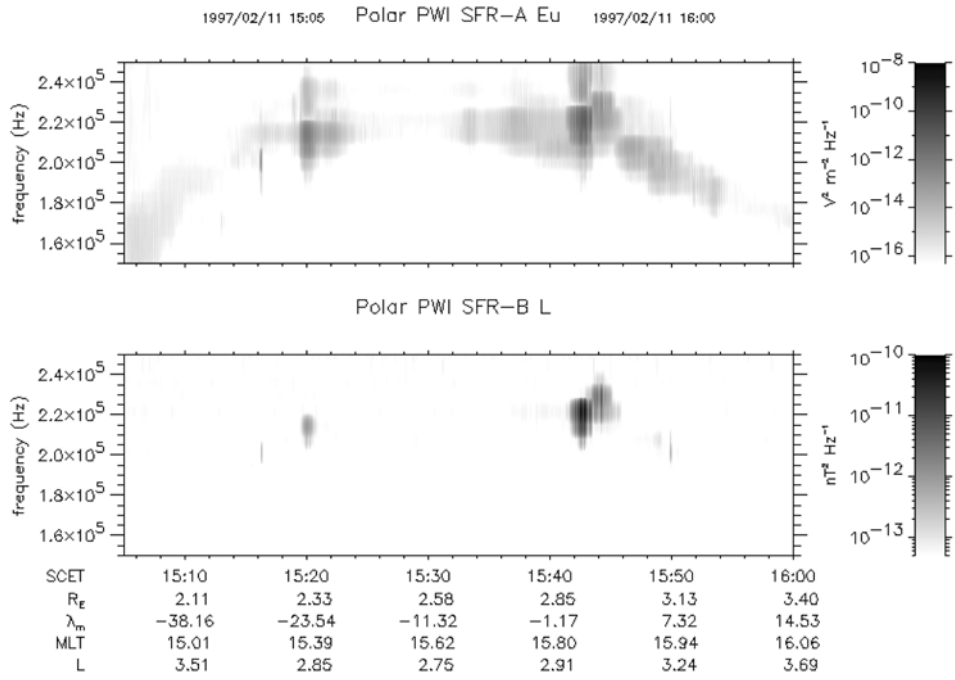

Figure 4a. In Figure 4a we show a spectrogram of Polar SFR data for a 55-min period on day 11 February 1997. During this time period the spacecraft is located in the afternoon sector of MLT ranging from 15.0 hours to 16.1 hours. The radial distance varies from 2.11 R_E to 3.4 R_E. Significantly, the magnetic latitude varies from high southern latitudes, $-38.2°$ through the magnetic equator to $\sim 14.4°$.

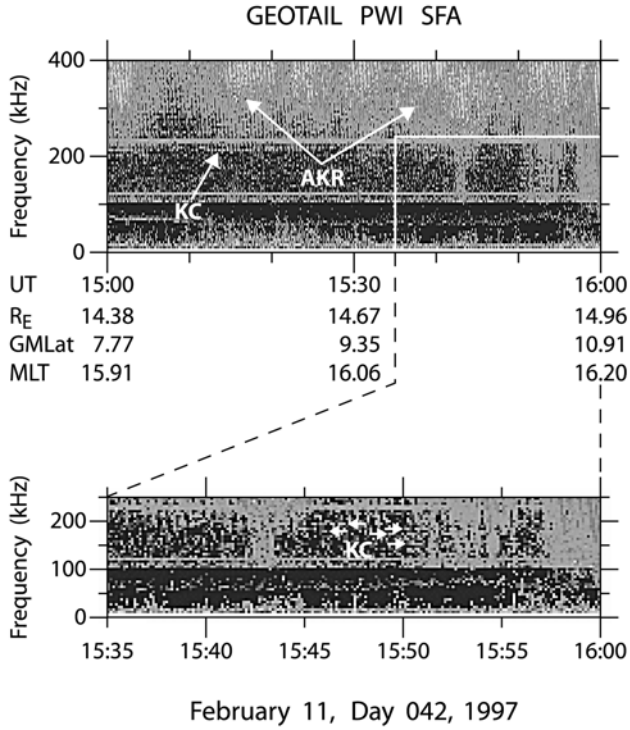

Figure 4b. Geotail spectrogram for a time interval close to that of Figure 4a. The KC emission is indicated and is superposed by intense AKR. The blow-up shows the KC emission at higher resolution as the monochromatic structures (note arrows).

the range 3.1 R_E < R < 3.7 R_E, $-4.9° < \lambda_m < 7.75°$, and 21.9 hours < MLT < 22 hours. Thus Polar is about 8 hours away in MLT. It would be unlikely that a plasmaspheric density notch would extend in longitude for this range. Owing to refractive effects of the high-density plasmasphere it would seem unlikely that O-mode emission with a source near Polar would be observed at the location of Geotail unless there were an extensive density cavity along the ray path between the two satellites. In Figure 6 we observe several bands of UH emission in the electric field data and a few bands of EM emission in the magnetic field data of the lower panel. The bands of emission are separated by ~20 kHz, consistent with the local value of f_{ce} which, during this time period, lies in the range 16 kHz < f_{ce} < 24 kHz. Spin modulation is clearly seen in the Polar data and analyses of the antenna orientations relative to the local ambient magnetic field give results consistent with those for the data of 20 May 1996, shown in Figure 3a. The electric field data are consistent with UH emission while the magnetic data are out of phase by 90° in spacecraft rotation and thus indicate possible Z-mode and ordinary mode emission. The magnetic field data for the time interval of Figure 6 are particularly intense, and we have calculated the ratio of B/E for a large fraction of this interval. These ratios vary considerably with frequency and time, but intermittently throughout this period have values <1 indicative of (but not positively identifying) nearly pure Z, O, or X mode emission.

[17] In Figure 7a we show an example of Polar SFR data for 15 May 1996. The spacecraft is located in the range $3.8 < R < 5.3\ R_E$, $-7.0° < \lambda_m < 13.2°$, and MLT ~22.3 hours. The interesting aspect of this data is the clear and rapid decrease in frequency of the UH signature (centered near 1751) in both the electric and magnetic field indicating a

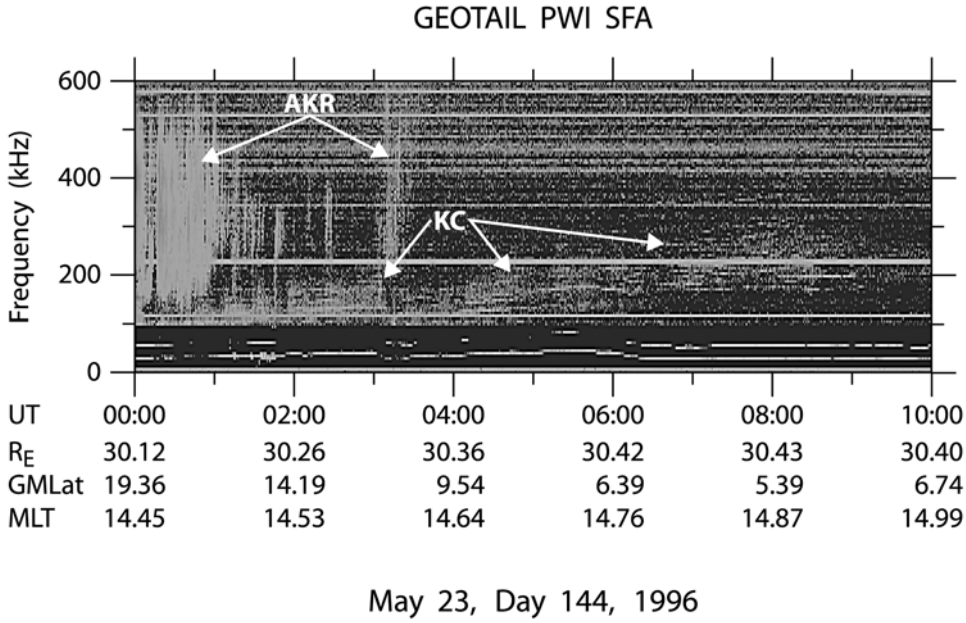

Figure 5a. In Figure 5a we show Geotail observations for a 10 hour period of 23 May 1996. Polar observations for the period from 0210 to 0232 are compared in Figure 6. We note that Geotail at this time is located at R ~ 30.25 R_E, MLT ~ 14.55 hours, and $\lambda_m \sim 13°$, while Polar was in the range 3.1 R_E < R < 3.7 R_E, $-4.9° < \lambda_m < 7.75°$, and 21.9 hours < MLT < 22 hours. Thus the MLT of Polar is about 8 hours different from that of Geotail.

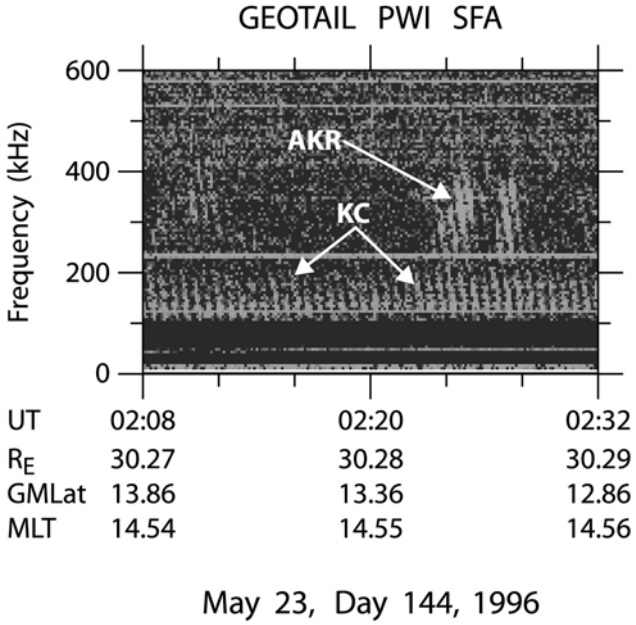

Figure 5b. Geotail wave data at a higher resolution for comparison with Figure 6. We note the KC emission showing a spin modulation in the frequency range from 100 kHz < f < 200 kHz.

probable density fluctuation, perhaps due to the spacecraft crossing a density duct or encountering a density cavity. The orbit of Polar varies essentially only in latitude at this time and very little in azimuth or L-shell. We do not discount, however, that Polar could be encountering a plasmaspheric notch at this time. At this same time period, Geotail detected clear signatures of KC emission over the frequency range 100 kHz < f < 800 kHz, but the spacecraft was located on the dayside near 9 hours MLT. The Geotail data for a similar time interval is shown in Figure 7b with KC emission particularly in the frequency range 100 kHz < f < 200 kHz. Again, due to the large azimuthal separation of Polar and Geotail, it is unlikely that the KC emission observed by Geotail is the same emission as observed by Polar. This example of isolated, significant decreases of the frequency of the UH emission in the Polar wave data is certainly not unique. Numerous other examples with corresponding EM emission have been discovered in the Polar PWI data.

[18] The high-resolution wideband data of the Polar PWI is not often available during magnetic equator crossings. However, on 10 April 1996, we were fortunate to have a time interval in which the instrument was operating in the correct frequency range. In Figure 8 we show the spectrogram of the data from the SFR. This data looks typical of many of the other crossings of the magnetic equator, this time located at MLT $\sim$ 0.35 and R $\sim$ 4.5 R_E. There is some rather intense electric field emission and faint but distinct magnetic oscillations observed in the interval from about 1527 to 1533. In Figure 9 we show the electric field wideband receiver data for a 48-s time interval starting at 1530:46. This data covers a frequency range from 125 kHz to about 215 kHz, which includes the EM emission seen in Figure 8. Of particular significance in Figure 9 are the many relatively intense near-constant frequency emission bands observed. In the frequency range 150 kHz < f < 170 kHz the separation of the bands is in the range of 2 to 3 kHz, whereas the spacing is even less for f > 170 kHz. There is

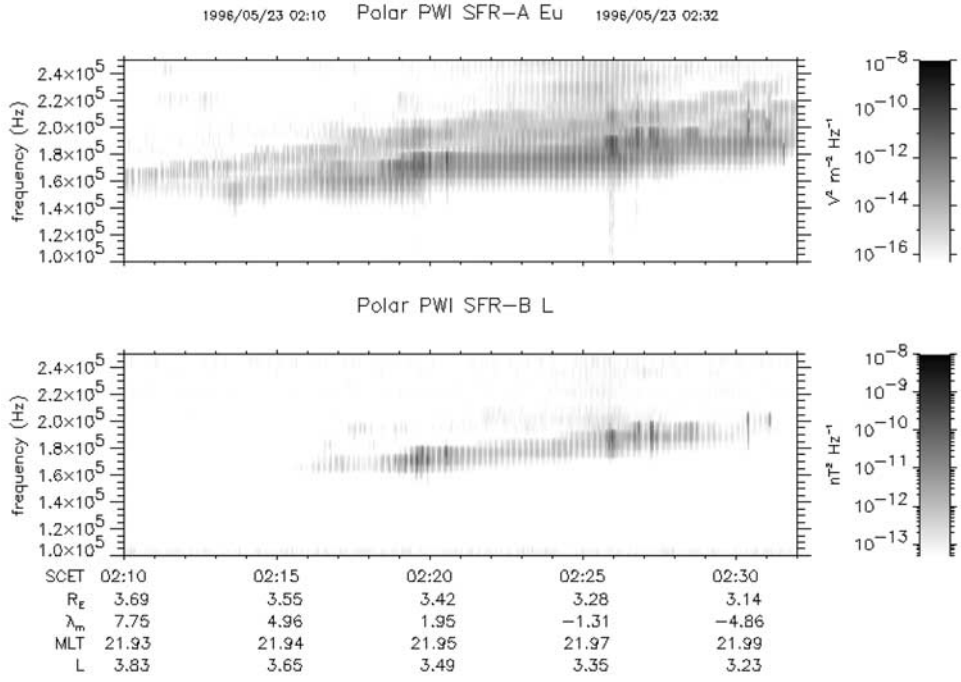

Figure 6. Electric and magnetic field data observed by Polar for a time period similar to that of Figure 5b (Geotail). We observe several bands of UH emission in the electric antenna and a few bands of EM emission in the magnetic field data of the lower panel. Spin modulation is clearly seen in the Polar data which allows us to speculate on the wave modes present.

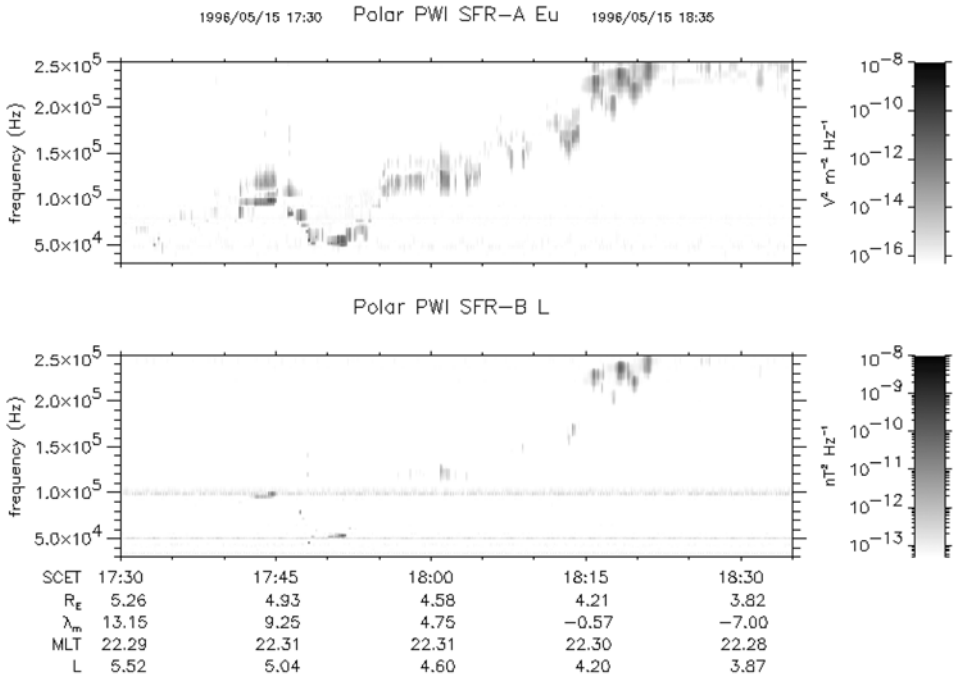

Figure 7a. We show an example of Polar SFR data for 15 May 1996. The spacecraft is located in the range $3.8 < R < 5.3\ R_E$, $-7.0° < \lambda_m < 13.2°$, and MLT ~22.3 hours. The interesting aspect of this data is the clear oscillation of the UH signature in both the electric and magnetic field indicating a probable density fluctuation, perhaps due to the spacecraft crossing a density duct or encountering a density cavity. In the magnetic field data (lower panel) we note the electromagnetic nature of the emission. Interference lines are located at $f = 50$ kHz, and $f = 100$ kHz.

also a spin modulation observed in the data showing nulls at ~3 s intervals. This modulation is consistent with electrostatic UH emission for the most intense bands in the interval $150 \text{ kHz} < f < 170$ kHz. We note, however, that the emission at higher frequencies, $f \geq 190$ kHz, shows emission maxima and nulls that are ~90° out of phase relative to the lower frequency emission. This indicates emission consistent with the ordinary mode. The local electron cyclotron frequency at this time is about 9 kHz and is much larger than the approximate separation of the bands seen in Figure 9. Therefore these bands most likely do not represent harmonics of local f_{ce}. This implies that each band of emission has a different source region.

[19] The Cluster spacecraft orbit intercepts the magnetic equator near the plasmapause during 2002, and we were fortunate to have the plasma wave wideband instrument in a fortuitous operating mode on 19 June 2002. In Figure 10 we display a spectrogram of the wideband instrument for the SC2 spacecraft. The spectrogram covers a frequency range from 250 kHz to 260 kHz over a 30-s time interval. The spacecraft is located just above the magnetic equator at $\lambda_m \sim 3.2°$, $R = 4.36\ R_E$, and MLT ~ 17 hours. Seen in the figure are very many closely spaced emission bands that increase slightly in frequency over the 30 s period of the plot. Spin modulation lanes are also seen at about 2 s intervals (the Cluster spin period is approximately 4 s). Because of the limited data for this time interval, we are unable to definitively determine the wave mode of these emissions. The similarity between this plot and Figure 9 is striking. The difference is in the frequency resolution. While operating in the 10 kHz bandwidth mode, Cluster has a higher frequency resolution than the Polar wideband instrument and is capable of detecting emission differences of ~100 Hz in this frequency range. In Figure 10 the band separations discernable are only a few hundred Hz and perhaps smaller. The electron cyclotron frequency for this time period is approx-

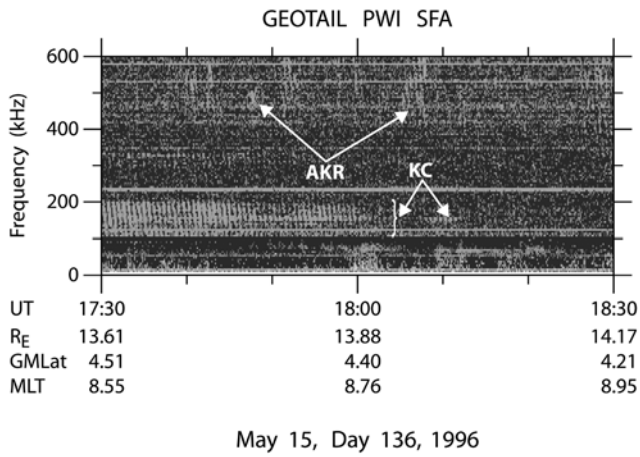

Figure 7b. Geotail wave spectrogram for approximately the same time period as that of Figure 7a. Note the presence of some KC emission. The Geotail spacecraft and the Polar spacecraft are well separated in azimuth at this time.

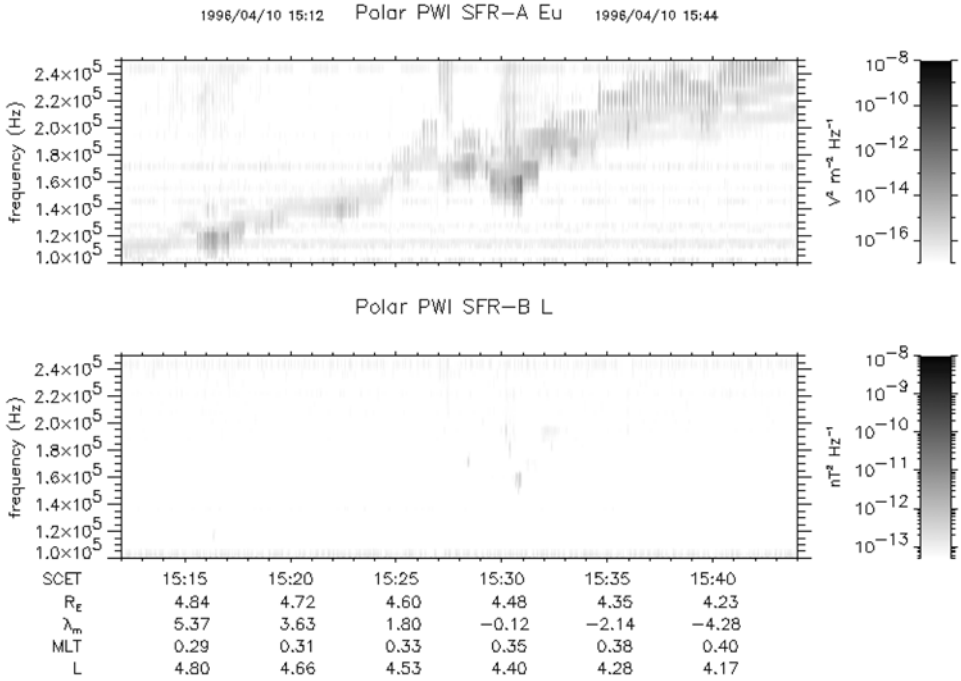

Figure 8. Polar SFR spectrogram for a magnetic equator crossing on 10 April 1996. This data looks typical of many of the other crossings of the magnetic equator, this time located at MLT $\sim$ 0.35 and R $\sim$ 4.5 R_E. There is some rather intense electric field emission and faint but distinct magnetic oscillations observed in the interval from about 1527 to 1533.

imately 10 kHz so that the bands of Figure 10 are much too close to represent harmonics of f_{ce}.

4. Summary and Conclusions

[20] We have presented plasma wave data from three satellites that suggest kilometric continuum emission has a source in the low-latitude plasmasphere as has been argued by *Hashimoto et al.* [1999]. The Polar spacecraft orbit allowed direct observation of magnetic equator crossings in the range of distances from $\sim$2.5 R_E (dayside) to $\sim$4.5 R_E (nightside) during 1996 and 1997. On many passes Polar observed upper hybrid emission near the higher density regions in the vicinity of the magnetic equator as has been reported often in the past [cf. *Kurth*, 1982; *Oya et al.*, 1991] and as discussed earlier in the Introduction. Often this emission was accompanied by EM emission detected by the magnetic receiver of the Polar PWI. On numerous passes, this emission was observed simultaneously with Geotail observations of kilometric continuum, when Geotail and Polar were near the same MLT and both close to the magnetic equator. Other similar EM observations were made when Polar and Geotail were well separated in MLT. The Polar SFR observations are typically banded with separations in frequency consistent with the local electron cyclotron frequency. Spin modulation observed by the Polar observations indicate the electric field emission is consistent with UH waves, and the magnetic oscillations are consistent with Z or ordinary mode emission.

[21] *Green et al.* [2002a, 2002b] have reported that kilometric continuum appears to have a source within the plasmasphere density notch or bite-out region, but they clarify that such regions may not be a necessary condition for KC emission. These regions have been detected in images obtained from the extreme ultraviolet (EUV) imager on board the IMAGE satellite which was launched in 2001. As reported by *Green et al.* [2002a] these notch regions are of large scale with extents of perhaps 10° to 15° with density depletions of perhaps 90% of the local nominal value. Our Polar observations cannot confirm that the EM emission is within a density notch, but several observations of oscillating frequency of UH emission indicate fluctuations in local density values of a somewhat smaller size scale, such as those seen in Figure 7a. The simultaneous observations of Polar and Geotail, when the two spacecraft are well separated, could only be associated with a plasmaspheric density notch if there was more than one notch in the plasmasphere at the time. It is also interesting to note that Polar PWI observed EM emission within the plasmasphere at relatively high latitude, well above the ±10° range found for most KC by *Hashimoto et al.* [1999] (cf. 11 February observations of Figure 2a).

[22] If the EM emissions observed by Polar are KC that is identified in the Geotail spectrograms, then our results indicate that KC emission is not necessarily confined to plasmaspheric notch regions. This is true because Polar observed this emission typically as it neared the magnetic equator, independent of the location of Geotail. Unless the plasmaspheric notches are much more common than observations to date imply, then Polar observations imply that the presence of a density notch is not necessary for the generation KC as also suggested by *Green et al.* [2002a]. However, the notch may focus the KC emission via refraction so that it is more easily detected by a remote satellite

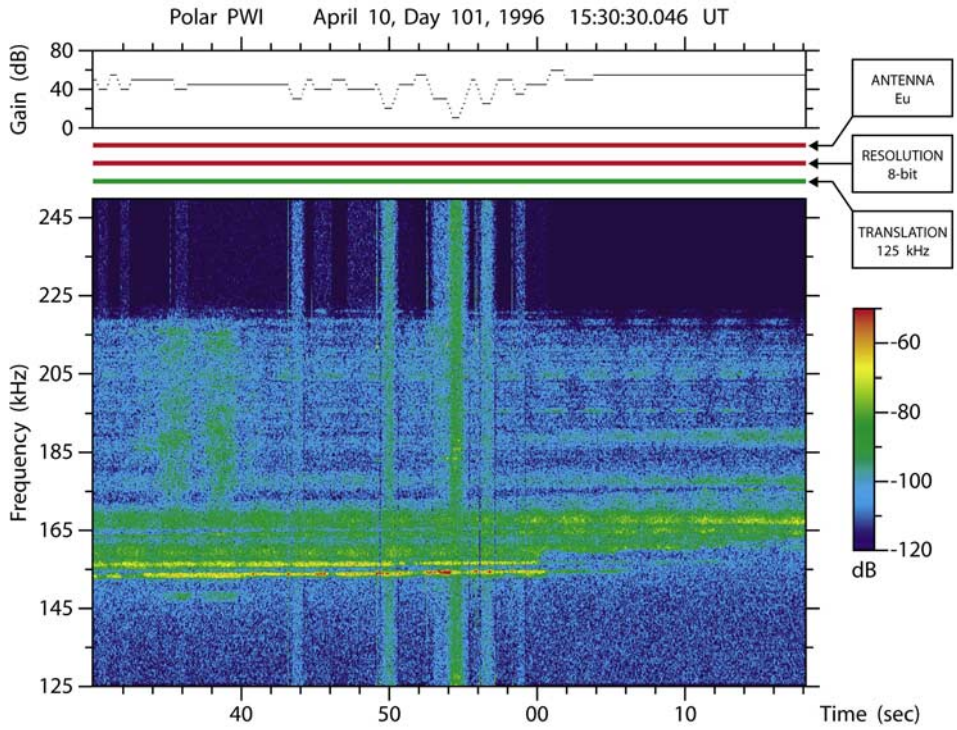

Figure 9. Spectrogram of the high resolution wideband receiver electric field data for a 48-s time interval starting at 1530.046 on 10 April 1996. This data covers a frequency range from 125 kHz to about 215 kHz, which includes the EM emission seen in Figure 8. Of particular significance are the many relatively intense near-constant frequency emission bands. The frequency separation of these bands is much less than the local electron cyclotron frequency. There is also a spin-modulation of the data showing nulls at ~3 s intervals. This modulation is consistent with electrostatic UH emission for the most intense bands in the interval 150 kHz < f < 170 kHz. For f > 190 kHz the emission nulls are ~90° out of phase with those for f < 190 kHz, and are consistent with ordinary mode emission.

[cf. *Green et al.*, 2002a]. We have been able to confirm that Image EUV data indicates that there is a good possibility that the Cluster spacecraft was located in or near a plasmaspheric notch during the observations of Figure 10 (D. Gallagher, private communication, 2003). This does not prove that the emission is KC but does suggest that KC would be expected to be observed at this time and location.

[23] The wideband observations of Polar and Cluster provide new and interesting information. Multiple closely spaced (in frequency) bands observed by both spacecraft near the magnetic equator and within the plasmasphere indicate that the emission is not just due to harmonics of f_{ce}. One explanation for such emission is that it is due to multiple UH sources or ordinary mode emission from source regions located at different radial distances (hence frequency). Each narrow-banded emission may have a different source location. A radial separation of <1000 km could explain differences of f_{ce} of only a few hundred Hz. If some of the lines observed in Figures 9 and 10 are due to UH resonances or Z-mode emission, then density fluctuations would also be important because $f_{UH} = \sqrt{(f_p^2 + f_{ce}^2)}$, where f_p is the plasma frequency. It is conceivable that density fluctuations in the form of cavities or ducts (enhancements) may be present. Each band of emission could have a different source region and therefore a different local plasma frequency. One cannot assume that all of the lines correspond to a single value of f_p, otherwise the frequency range, 150 kHz < f < 170 kHz, observed in Figure 9 for instance, would imply UH emission at frequencies less than the low-frequency cutoff. Another possibility is that the closely spaced emission lines represent trapped emission resonating inside closely spaced density fluctuations. The electrostatic emission is converted to electromagnetic emission by some process as suggested below. Density cavities have recently been reported by P. Decreau (private communication, 2002) by the Cluster WAVES experiment [e.g., *Moullard et al.*, 2002]. Eigenmode trapping of Langmuir waves in density cavities and Z-mode emissions in density enhancements [cf. *McAdams et al.*, 2000; *Yoon et al.*, 2000] have been suggested to explain discrete emissions (fine structure) of auroral HF chirps and auroral roar, respec-tively. A modification of such processes might also explain the present observations.

[24] To briefly elaborate, auroral roar emissions are believed to be due to quasi-electrostatic Z-mode (or upper hybrid) waves that are partly converted to free-space radio waves (auroral roar) and observed on the ground. *Yoon et al.* [2000] have performed WKB-type calculations of the discrete frequency eignemodes that result from upper hybrid waves trapped in a density enhancement region. Using parameters that are appropriate for the auroral region (but not the plasmapause) the authors solve the dispersion relation and demonstrate that a spectrum of electrostatic emission with frequency separations typical of auroral roar

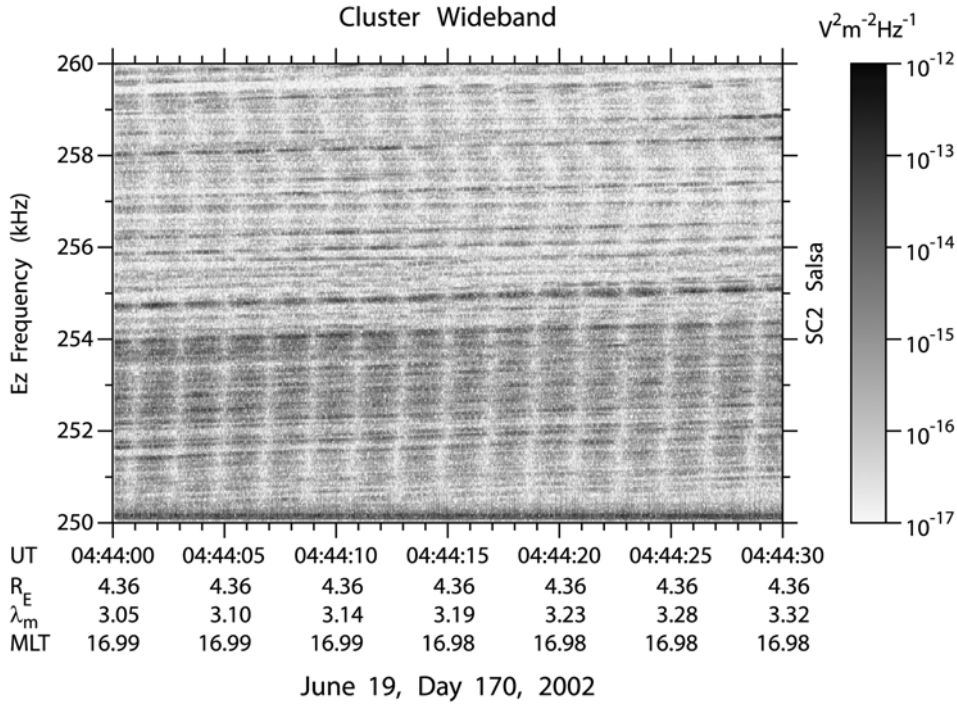

Figure 10. A spectrogram of electric field data obtained by the wideband instrument (WBD) on board the Cluster (SC2) spacecraft on 19 June 2002. The spectrogram covers a frequency range from 250 kHz to 260 kHz over a 30-s time interval. SC2 is located just above the magnetic equator at $\lambda_m \sim 3.2°$, R = 4.36 R_E and MLT $\sim$ 17 hours. Seen in the figure are very many closely-spaced emission bands that increase slightly in frequency over the 30 s period of the plot. Spin modulation lanes are also seen at about 2 s intervals. The similarity between this plot and Figure 9 is striking.

observations can be predicted. It is easy to see how this theory may be applied to the generation of kilometric continuum. Density irregularities and enhancements or ducts have been observed near the plasmapause by many authors [cf. *LeDocq et al.*, 1994]. It will be interesting to extend the theory of *Yoon et al.* [2000] to the parameter domain of the terrestrial plasmasphere to confirm that density ducts may be the source of the observed kilometric continuum fine structure. To explain the overlapping fine structure observed in Figures 9 and 10 one can envision emission from a number of density ducts along adjacent or closely-spaced magnetic field lines.

[25] In earlier work to explain the generation of auroral roar, *Yoon et al.* [1998] have shown that the growth rates of Z-mode are greatly enhanced when $f_{UH}^2 = f_{ce}^2 + f_{pe}^2 = (nf_{ce})^2$, where n = 2 and 3. This Z-mode can escape into free space by a linear mode conversion into the O or whistler mode [e.g., *Ellis*, 1956]. *Willes et al.* [1998] investigated a competing theory of nonlinear coalescence to explain the conversion of Z-mode to a freely propagating mode (cf. *Melrose* [1991] applied to solar radio emission). Some details of each of these theories have yet to be published. It is probable, however, that such ideas may apply directly to the generation of kilometric continuum emission. These theories are closely related to those already suggested for kilometric continuum by investigators mentioned in the Introduction.

[26] The source mechanism of KC emission is probably the same as that of the terrestrial and planetary non-thermal continuum [cf. *Kurth*, 1992], which has been generally described by the linear conversion theory of *Jones* [1988] or by the nonlinear conversion mechanisms described by *Melrose* [1981], *Barbosa* [1982], or *Rönnmark* [1983, 1989, 1992]. All of these mechanisms involve upper hybrid waves. In the linear mechanism UH waves refract (in a steep density gradient) to Z-mode waves at a wave normal angle near 90°. Z-mode waves can mode convert to O-mode waves [cf. *Horne*, 1989, 1990]. The nonlinear mechanisms are described by the authors as more efficient than the linear conversion mechanism. For these processes, UH waves coalesce with some lower-frequency wave. The polarization and wave modes obtained by Polar are consistent with these theories, but we cannot easily distinguish between them. It is hoped that future Cluster observations may help resolve some of these outstanding questions regarding the source of KC.

[27] **Acknowledgments.** The authors thank J. Hospodarsky for text editing and A. Persoon for editing of the figures. The research at Iowa was supported by NASA grant NAG5-11942 and NAG5-9561. R. R. Anderson appreciates support for his participation in this research under his Visiting Professorship at RASC, Kyoto University, and at the University of Iowa by grant NAG5-11707 from NASA Goddard Space Flight Center.

[28] Lou-Chuang Lee thanks Dennis L. Gallagher and another reviewer for their assistance in evaluating this paper.

References

Barbosa, D. D., Low-level VLF and LF radio emissions observed at Earth and Jupiter, *Rev. Geophys.*, *20*, 316–334, 1982.

Brown, L. W., The galactic radio spectrum between 130 kHz and 2600 kHz, *Astrophys. J.*, *180*, 359–370, 1973.

Budden, K. G., The theory of radio windows in the ionosphere and magnetosphere, *J. Atmos. Terr. Phys.*, *42*, 287–298, 1980.
Ellis, G. R., The *Z* propagation hole in the ionosphere, *J. Atmos. Terr. Phys.*, *8*, 43, 1956.
Fung, S. F., and K. Papadopoulos, The emission of narrow-band Jovian kilometric radiation, *J. Geophys. Res.*, *92*, 8579–8593, 1987.
Green, J. L., B. R. Sandel, S. F. Fung, D. L. Gallagher, and B. W. Reinisch, On the origin of kilometric continuum, *J. Geophys. Res.*, *107*(A7), 1105, doi:10.1029/2001JA000193, 2002a.
Green, J. L., S. Boardsen, S. F. Fung, H. Matsumoto, K. Hashimoto, R. R. Anderson, B. R. Sandel, and B. W. Reinisch, Association of kilometric continuum radiation with plasmaspheric structures, *J. Geophys. Res*, in press, 2002b.
Gurnett, D. A., The Earth as a radio source: Terrestrial kilometric radiation, *J. Geophys. Res.*, *79*, 4227–4238, 1974.
Gurnett, D. A., The Earth as a radio source: The nonthermal continuum, *J. Geophys. Res.*, *80*, 2751–2763, 1975.
Gurnett, D. A., and R. R. Shaw, Electromagnetic radiation trapped in the magnetosphere above the plasma frequency, *J. Geophys. Res.*, *78*, 8136–8149, 1973.
Gurnett, D. A., et al., The polar plasma wave instrument, *Space Sci. Rev.*, *71*, 597–622, 1995.
Gurnett, D. A., et al., First results from the Cluster wideband plasma wave investigation, *Ann. Geophys.*, *19*, 1259–1272, 2001.
Hashimoto, K., W. Calvert, and H. Matsumoto, Kilometric continuum detected by Geotail, *J. Geophys. Res.*, *104*, 28,645–28,656, 1999.
Horne, R. B., Path-integrated growth of electrostatic waves: The generation of terrestrial myriametric radiation, *J. Geophys. Res.*, *94*, 8895–8909, 1989.
Horne, R. B., Narrow-band structure and amplitude of terrestrial myriametric radiation, *J. Geophys. Res.*, *95*, 3925–3932, 1990.
Jones, D., Source of terrestrial non-thermal continuum radiation, *Nature*, *260*, 686–689, 1976.
Jones, D., Planetary radio emissions from low magnetic latitudes: Observations and theories, in *Planetary Radio Emissions II*, edited by H. O. Rucker, S. J. Bauer, and B.-M. Pedersen, pp. 255–293, Austrian Acad. of Sci., Vienna, Austria, 1988.
Kurth, W. S., Detailed observations of the source of terrestrial narrowband electromagnetic radiation, *Geophys. Res. Lett.*, *9*, 1341–1344, 1982.
Kurth, W. S., Continuum radiation in planetary magnetospheres, in *Planetary Radio Emissions III*, edited by H. O. Rucker, S. J. Bauer, and M. L. Kaiser, pp. 329–350, Austrian Acad. of Sci., Vienna, 1992.
Kurth, W. S., D. A. Gurnett, and R. R. Anderson, Escaping nonthermal continuum radiation, *J. Geophys. Res.*, *86*, 5519–5531, 1981.
LeDocq, M. J., D. A. Gurnett, and R. R. Anderson, Electron number density fluctuations near the plasmapause observed by CRRES spacecraft, *J. Geophys. Res.*, *99*, 23,661–23,671, 1994.
Matsumoto, H., I. Nagano, R. R. Anderson, H. Kojima, K. Hashimoto, M. Tsutsui, T. Okada, I. Kimura, Y. Omura, and M. Okada, Plasma wave observations with Geotail spacecraft, *J. Geomagn. Geoelectr.*, *46*, 59–95, 1994.
McAdams, K. L., R. E. Ergun, and J. LaBelle, HF chirps: Eigenmode trapping in density depletions, *Geophys. Res. Lett.*, *27*, 321–324, 2000.
Melrose, D. B., A theory for the nonthermal radio continua in the terrestrial and Jovian magnetospheres, *J. Geophys. Res.*, *86*, 30–36, 1981.
Melrose, D. B., Emission at cyclotron harmonics due to coalescence of *z*-mode waves, *Astrophys. J.*, *380*, 256, 1991.
Morgan, D. D., and D. A. Gurnett, The source location and beaming of terrestrial continuum radiation, *J. Geophys. Res.*, *96*, 9595–9613, 1991.
Moullard, O., A. Masson, J. Laakso, M. Parrot, P. Décréau, O. Santolik, and M. Andre, Density modulated whistler mode emissions observed near the plasmapause, *Geophys. Res. Lett.*, *29*(20), 1975, doi:10.1029/2002GL015101, 2002.
Oya, H., M. Iizima, and A. Morioka, Plasma turbulence disc circulating the equatorial region of the plasmasphere identified by the plasma wave detector (PWS) on board the Akebono (EXOS-D) satellite, *Geophys. Res. Lett.*, *18*, 329–332, 1991.
Pedersen, A., et al., The wave experiment consortium (WEC), *Space Sci. Rev.*, *79*(1–2), 93–105, 1997.
Rönnmark, K., Emission of myriametric radiation by coalescence of upper hybrid waves with low frequency waves, *Ann. Geophys.*, *1*, 187–192, 1983.
Rönnmark, K., Myriametric radiation and the efficiency of linear mode conversion, *Geophys. Res. Lett.*, *16*, 731–734, 1989.
Rönnmark, K., Conversion of upper hybrid waves into magnetospheric radiation, in *Planetary Radio Emissions III*, edited by H. O. Rucker, S. J. Bauer, and M. L. Kaiser, pp. 405–417, Austrian Acad. of Sci., Vienna, 1992.
Willes, A. J., S. D. Bale, and Z. Kuncic, A *z* mode electron-cyclotron maser model for bottomside ionospheric harmonic radio emissions, *J. Geophys. Res.*, *103*, 7017–7026, 1998.
Yoon, P. H., A. T. Weatherwax, T. J. Rosenberg, J. LaBelle, and S. G. Shepherd, Propagation of medium frequency (1–4 MHz) auroral radio waves to the ground via the *Z*-mode radio window, *J. Geophys. Res.*, *103*, 29,267–29,275, 1998.
Yoon, P. H., A. T. Weatherwax, and J. LaBelle, Discrete electrostatic eigenmodes associated with ionospheric density structure: Generation of auroral roar fine frequency structure, *J. Geophys. Res.*, *105*, 27,589–27,596, 2000.

R. R. Anderson, D. A. Gurnett, J. D. Menietti, and J. S. Pickett, Department of Physics and Astronomy, University of Iowa, Iowa City, IA 52242, USA. (roger-r-anderson@uiowa.edu; donald-gurnett@uiowa.edu; jdm@space.physics.uiowa.edu; pickett@uiowa.edu)

H. Matsumoto, Radio Science Center for Space and Atmosphere, Kyoto University, Uji 611-0011, Japan. (matsumot@kurasc.kyoto-u.ac.jp)